A COMPACT LINEAR TAPERED SLOT ANTENNA WITH INTEGRATED BALUN FOR UWB APPLICATIONS

J. N. Wu[1], Z. Q. Zhao[1, *], J. Z. Liu[1], Z. P. Nie[1], and Q.-H. Liu[2]

[1]School of Electronic Engineering, University of Electronic Science and Technology of China, Chengdu 611731, China

[2]Department of Electrical and Computer Engineering, Duke University, Durham, NC 27708, USA

Abstract—A compact linear tapered slot antenna with wideband performance is proposed. The antenna consists of a microstrip to slotline transition and a linear tapered slot structure which is connected to the slotline. Due to the linear tapered slot, the antenna can realize unidirectional radiation in wideband band. The microstrip to slotline transition is implemented by using a tapered cross, which can easily obtain impedance transformation. Furthermore, this transition can be realized with a small size. The antenna is fabricated and optimized numerically. Both simulated and measured results validate the performance of the antenna in frequency and time domains. The results show that the antenna achieves a bandwidth up to 118% from 2.6–10.1 GHz. The simulated time domain response of the antenna also shows its good performance in time-domain. The antenna can be well applied to ultra-wideband system.

1. INTRODUCTION

There are many wireless applications that satisfy different demands for continuous, convenient, and flexible access to up-to-date information. One of them is ultrawideband (UWB) technologies [1]. UWB communication systems have attracted great attention in the wireless world because of their advantages, including high speed data rate,

extremely low spectral power density, and high precision ranging [2–4]. Such systems require antennas able to operate across a very large bandwidth with consistent polarization and radiation pattern parameters over the interest band [13].

Many types of UWB antennas have been proposed, such as printed dipoles [5, 6], monopoles [7–9], slot antenna [10] and some other CPW-fed printed antennas [11]. Most of these antennas are omnidirectional with low gain. For some applications such as positioning, directional finding or other link to link communication, directional or quasi directional antenna with wideband performance is needed [12]. However, some multi-resonant wideband antennas, such as log-periodic antennas, will widen the narrow pulse in the time domain due to multiple reflections and large discontinuities within their structures [13]. These designs are not suitable for UWB applications.

Some directional antennas with wideband performance, such as horn antennas [14], tapered slot antennas [15, 16], have a large size which makes it difficult to be used in engineering. A small tapered slot antenna with a notched band was proposed for the wireless communications in [17]. This antenna needs a thick substrate, and the overall size is relatively large. Some other small directional antennas have also been designed [18, 19]. However, these antennas need a double side feed line. Meanwhile, the ground plane will have a big effect on the radiation. Some slot antennas were proposed to realize directional radiation and wideband [20, 21]. These antennas always need a balun to realize symmetrical exciting. Microstrip to slotline has been successfully used as a balun applied to feed the antenna [22, 25]. Designing a small balun with wideband performance is still a challenging issue.

In this paper, a UWB antenna is proposed and fabricated. This antenna consists of an integrated balun and a linear tapered slot antenna. The integrated balun based on a microstrip to slotline transition is applied to improve the matching performance. The traditional square crossing is replaced by a tapered cross. Therefore, the impedance transformation between the microstrip and slotline can be easily obtained without any stepped impedance matching stubs. This transformation has a wideband performance with a compact size. This balun can be well integrated to the tapered slot antenna.

The remainder of the paper is organized as follows. In Section 2, the configuration of the proposed tapered slot antenna with integrated balun is proposed. Simulated and experimental results are given in Section 3. Time domain response of the antenna is analyzed in Section 4. Conclusions are made in the final section.
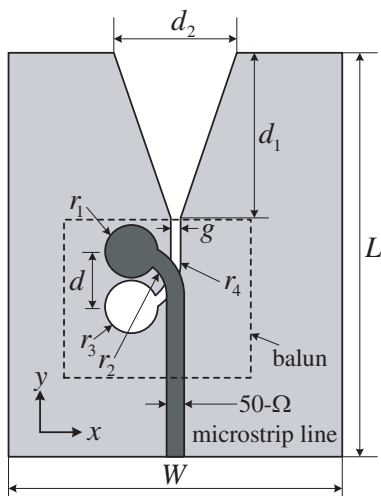
Figure 1. The configuration of the proposed antenna.

2. CONFIGURATION OF THE PROPOSED ANTENNA

The configuration of the proposed antenna is shown in Fig. 1. It consists of a microstrip to slotline and a linear tapered slot. The microstrip to slotline is composed of an open-circuited microstrip line and a short-circuited slotline. The radii of the circular disc patch and circular hole are r_1 and r_3, respectively. The radii of the quarter rings of microstrip line and the slotline are r_2 and r_4, respectively. The linear tapered slot is etched into the bottom of the substrate and connected to the slotline of the balun. The length and width of the linear tapered slot are d_1 and d_2, respectively.

In this design, the field matching between the microstrip mode and slotline mode is achieved by a virtual shorting caused by the open-circuited microstrip line with one circular disc patch. The impedance matching between the microstrip line and the slotline is realized by selecting proper values of the characteristic impedance of the slotline and the matching disc patch.

Due to the symmetrical currents on each edge of the slotline, the microstrip to slot transition can be used as an integrated balun, thus a feeding of the antenna. The open microstrip line and short-circuited slotline are printed on opposite sides of the substrate. Figs. 2(a) and (b) show the layout of the microstrip to the slotline transition structure and its equivalent circuit, respectively. As shown in Fig. 2(a), because the shorted slot is at the end of the slotline, the electromagnetic energy
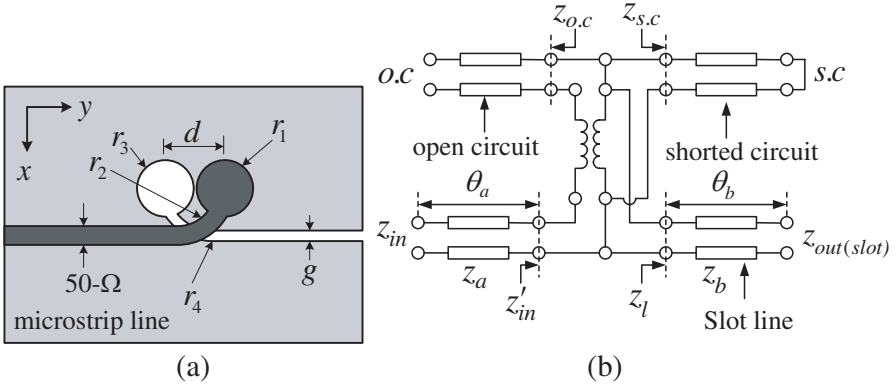
Figure 2. Microstrip to slotline transition line: (a) The layout and (b) the equivalent circuit.

is transferred from microstrip line to the slotline along with the y direction.

The impedance matching can be easily obtained by selecting proper values of the lengths of the open-circuited microstrip line and short-circuited slotline. Referring to [26], the slotline can be regard as a series loading of the microstrip. Assuming that the equivalent impendence at the end of the slotline is $z_{\text{out(slot)}}$, the equivalent input impedance z'_{in} shown in Fig. 2(b) is expressed as

$$z'_{\text{in}} = z_{o.c} + \frac{z_{s.c}z_l}{z_{s.c} + z_l}, \tag{1}$$

where z_a is the characteristic impedance, θ_a the electrical length of the microstrip line, z_l the equivalent impedance of the slotline, given as

$$z_l = z_b \frac{z_{\text{out(slot)}} + jz_b \tan\theta_b}{z_b + jz_{\text{out(slot)}} \tan\theta_b}, \tag{2}$$

where z_b and θ_b are the characteristic impedance and electrical length of the slotline, respectively.

In order to get proper values of the parameters shown in Fig. 2(a), a model is set up and simulated by a software CST Microwave Studio. The simulated results of the transition, in Fig. 3, show that the integrated balun has a wideband performance and a low insertion loss. In the band from 2–14 GHz, the return loss is less than -12 dB and the insertion loss less than 1 dB.

Based on the balun structure given in Fig. 2, Figs. 4(a) and (b) show the layout of the proposed antenna and its equivalent circuit.
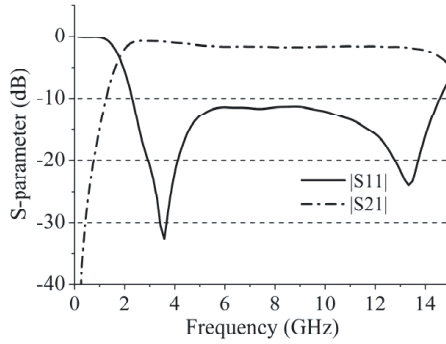
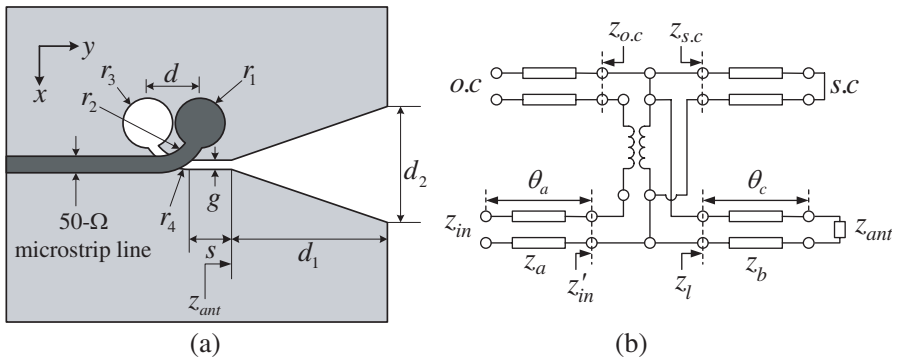**Figure 3.** Simulated S-parameters of the microstrip to slot transition.

Figure 4. The proposed antenna: (a) The layout and (b) the equivalent circuit.

The equivalent impedance is expressed as

$$z'_{\text{in}} = z_{o.c} + \frac{z_{s.c} z_b \frac{z_{\text{ant}} + j z_b \tan \theta_c}{z_b + j z_{\text{ant}} \tan \theta_c}}{z_{s.c} + z_b \frac{z_{\text{ant}} + j z_b \tan \theta_c}{z_b + j z_{\text{ant}} \tan \theta_c}}, \tag{3}$$

where θ_c is the electrical length of s shown in Fig. 4(a).

By selecting proper values of the lengths of the open-circuited microstrip line and short slotline, the equivalent impedance z'_{in} can be simplified as

$$z'_{\text{in}} = z_b \frac{z_{\text{ant}} + j z_b \tan \theta_c}{z_b + j z_{\text{ant}} \tan \theta_c}. \tag{4}$$

Therefore, the impedance matching of the proposed antenna will be improved by changing the length and characteristic impedance of the slotline. The model structure of the proposed antenna will be further discussed in the following section.

3. EXPERIMENTAL RESULTS AND DISCUSSIONS

The configuration of the antenna, proposed in Section 2, is simulated by using software CST Microwave Studio. The dielectric substrate is FR4 with a dielectric constant of 4.4 and thickness of 0.5 mm, respectively. The microstrip line has a characteristic impedance of 50 Ω, corresponding to a width of 0.9 mm. The optimized dimensions (in mm) are: $r_1 = 3.5$, $r_2 = 1.5$, $r_3 = 2.5$, $r_4 = 1.6$, $g = 0.4$, $s = 4$, $d = 3$, $d_1 = 12$, $d_2 = 8$. An antenna is fabricated with the these parameters. The manufactured antenna has an overall size of 38 mm × 32 mm. Fig. 5 shows the photographs of the antenna. A 50-Ω SMA connector is used to feed the antenna. The results of the simulations and measurements are compared in Figs. 6–7.

As shown in Fig. 6, the simulated impedance bandwidth is 7.6 GHz, from 2.6–10.2 GHz. The measured one is 7.5 GHz, from 2.6–10.1 GHz. The simulated and measured results agree very well.
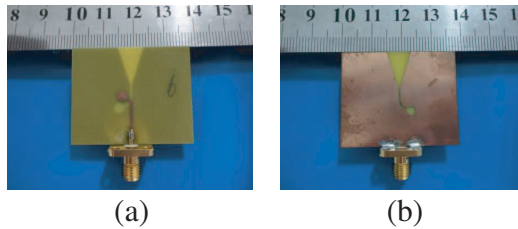

(a)   (b)

Figure 5. Photographs of the fabricated antenna. (a) The top side. (b) The bottom side.
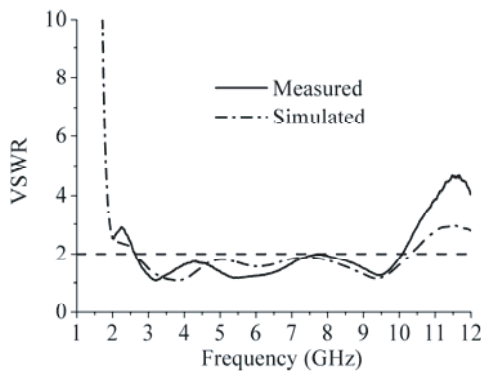

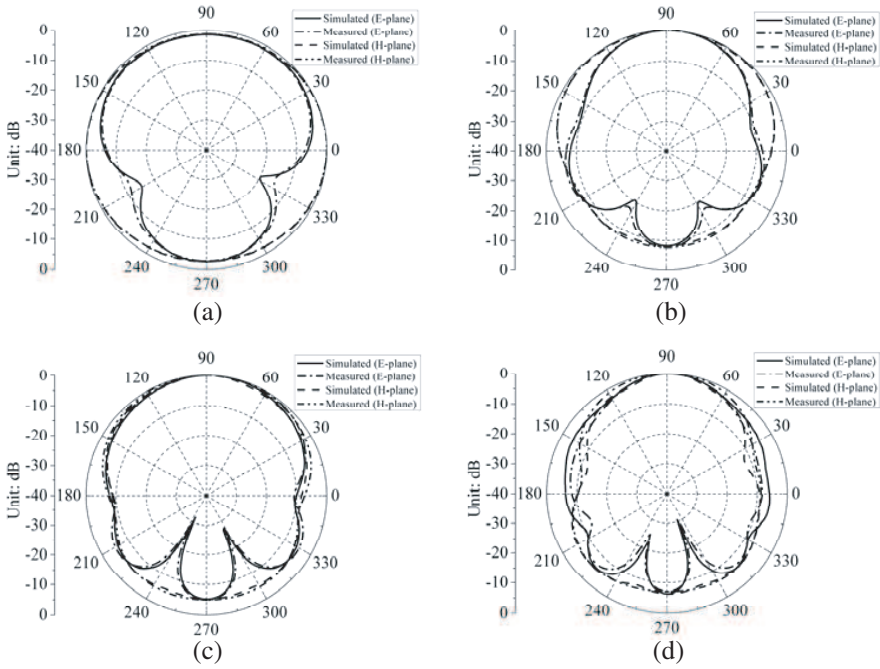**Figure 6.** The simulated and measured responses of VSWR of the antenna.

Figure 7. Simulated and measured radiation patterns of the proposed slot antenna in *E*-plane and *H*-plane at different frequencies. (a) 3.5 GHz. (b) 6 GHz. (c) 8 GHz. (d) 10 GHz.
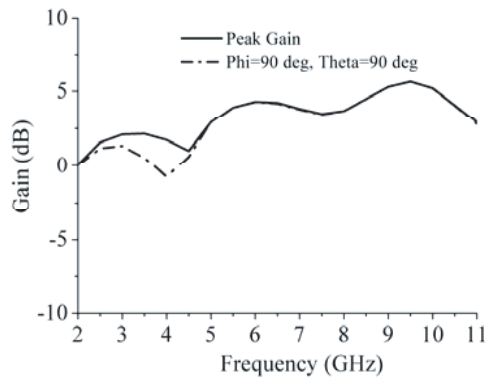

Figure 8. Measured peak gain and the gain in *y* direction of the antenna.

Figure 7 plots both E-and H-plane radiation patterns of the antenna for simulated and measured results at 3.5, 6, 8 and 10 GHz, respectively. As shown in the figures, the antenna has endfire characteristics with the main-direction in y direction of the tapered slot at high frequency band. The gain varying with the frequency is shown in Fig. 8. In the band 2–4.5 GHz, the gain in y direction is lower than the peak gain, because the radiation pattern of the proposed antenna at the lower frequency band is similar to that of a dipole antenna. In the band 4.5–11 GHz, the gain in y direction is close to the peak gain, which implies that the antenna has a stable radiation directivity in this frequency band.

4. TIME-DOMAIN RESPONSE

Time-domain response is an important feature of a pulsed radio communication system. As discussed in the previous section, the proposed antenna has a wide bandwidth. The center frequency of the proposed tapered slot antenna is at the 6.35 GHz with a 118% bandwidth. However, the wide band does not necessarily ensure its good performance in time-domain. The group delay will be unstable because the gain decreases substantially induced by some band-notched structures [27]. Thus the pulse will be changed in time-domain. Following similar methods as in [1, 23, 24], the time-domain response of the antenna is numerically studied.

The antenna is assumed to be excited by an UWB signal which covers 3.1–10.6 GHz. Fig. 9 shows the transmitted signal along with its Fourier transform. The time-domain performances of the proposed antenna are obtained by placing virtual probes at a distance of 700 mm from the antenna. The distance is set according to the far-field condition.
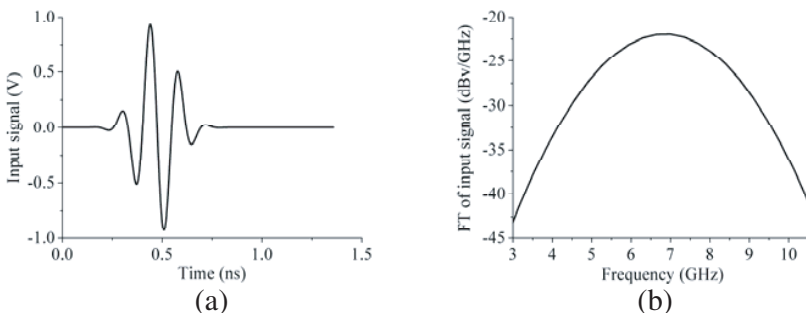

(a)   (b)

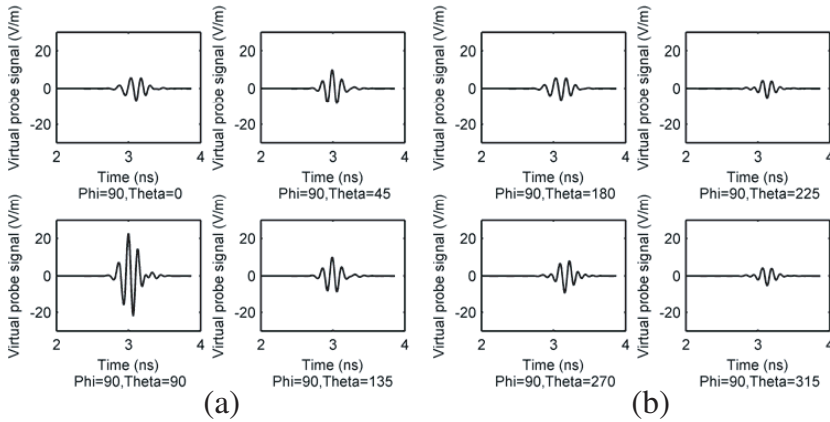**Figure 9.** Time domain and frequency domain of the input signal. (a) The input signal. (b) Fourier transform of the input signal.

Figure 10. Virtual probe signals of the proposed antenna in different angles. (a) $\varphi = 90°$, $\theta = 0°$, $45°$, $90°$, $135°$. (b) $\varphi = 90°$, $\theta = 180°$, $225°$, $270°$, $315°$.

Table 1. Field factor of the antenna in different angles.

Angle (°)	Value	Angle (°)	Value
$\varphi = 90$, $\theta = 0$	0.9362	$\varphi = 90$, $\theta = 180$	0.9217
$\varphi = 90$, $\theta = 45$	0.9560	$\varphi = 90$, $\theta = 225$	0.9036
$\varphi = 90$, $\theta = 90$	0.9596	$\varphi = 90$, $\theta = 270$	0.9137
$\varphi = 90$, $\theta = 135$	0.9520	$\varphi = 90$, $\theta = 315$	0.8870

Figure 10 shows the received signals of the virtual probes at different angles. The output signal of the proposed antenna at $\varphi = 90°$, $\theta = 90°$ is similar to the input signal with very tiny distortions. The output signals at other angles also have similar waveforms. In order to further determine the correlation coefficient between the output and input signals, the correlation coefficient is induced, expressed as [23]

$$\rho = \max_{\tau} \left\{ \frac{\int s_1(t)s_2(t - \tau)dt}{\sqrt{\int s_1^2(t)dt}\sqrt{\int s_2^2(t)dt}} \right\}, \qquad (5)$$

where $s_1(t)$ and $s_2(t)$ are input and output signals, respectively.

The values of the correlation coefficient obtained at different angles are summarized in Table 1. It is seen that the field factors of the proposed antenna in $\theta = 45°$, $90°$, $135°$ are close to 1.0 when $\varphi = 90°$. The output signals at these angles are very similar to the input signal.

Figure 11 shows the peak-peak values of the virtual probe signals at different angles. It is seen that the peak-peak value has a maximum value of $45\,\mathrm{V/m}$ at $\varphi = 90°$, $\theta = 90°$. The peak-peak values at other angles are lower than $20\,\mathrm{V/m}$, which implies that this antenna has a good directional radiation in time domain.
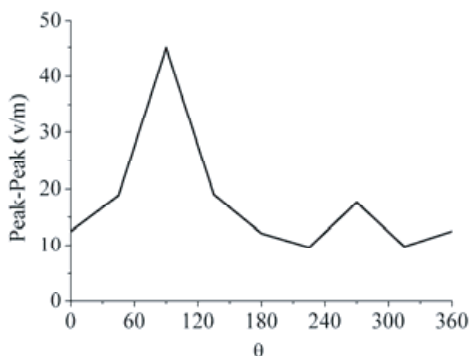

Figure 11. Peak-peak values of the virtual probe signals in different angles with $\varphi = 90°$.
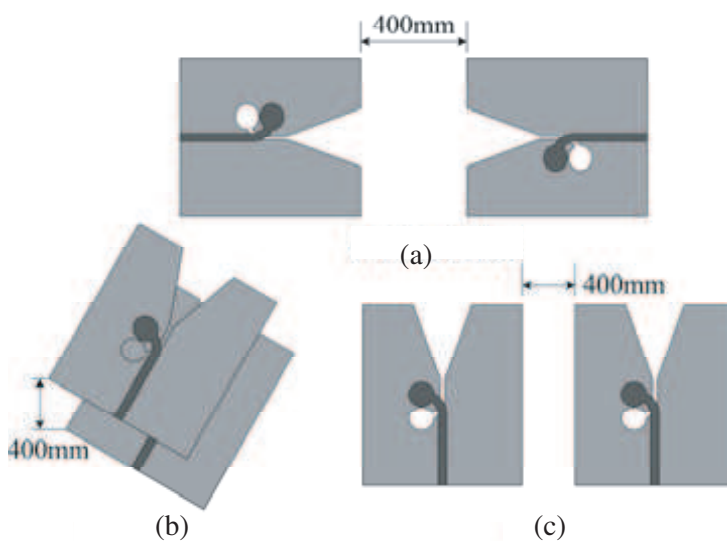

Figure 12. The communication link established of the antennas in different types: (a) Face to face. (b) Face to side. (c) Side to side.
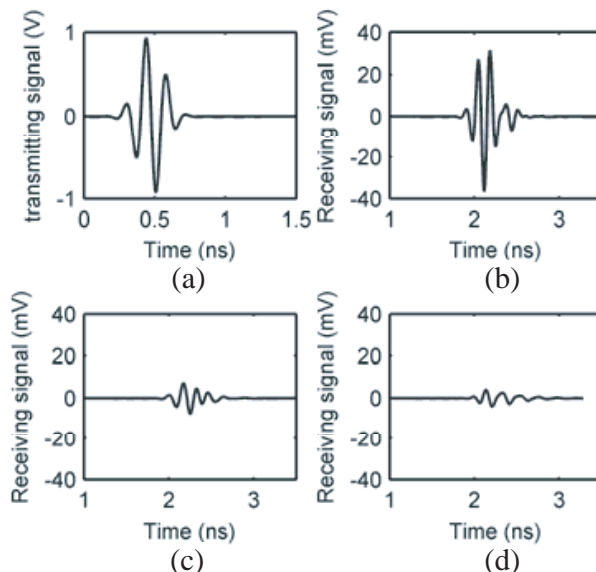
Figure 13. Receiving signals of the antennas in different types: (a) Input signal. (b) Face to face. (c) Face to side. (d) Side to side.

Table 2. The correlation coefficient and the peak-peak values of the receiving signals.

Type	Correlation Coefficient	Peak-Peak Value
face to face	0.9315	67 mV
face to side	0.8879	14 mV
side to side	0.7467	8 mV

In order to further verify the time-domain response, two identical antennas are placed at different positions as shown in Fig. 12. The communication link is established by the antennas placed in free space. The distance between the transmitting and receiving antennas is assumed to be 400 mm. The received signals of the antennas at different types are shown in Fig. 13. The correlation coefficient and peak-peak value are given in Table 2. As shown in Fig. 13, it is seen that the received signals do not change too much at the main direction when the antennas is placed face to face. The correlation coefficient between the transmitting and receiving signals is about 93%. Thus the antenna can be well applied to ultra-wideband system.

5. CONCLUSION

A compact linear tapered slot antenna with wideband performance
is proposed. The antenna consists of a linear tapered slot structure
and a microstrip to slotline transition. The linear tapered slot
structure is connected to the slotline. The features of the antennas
are both theoretically and experimentally studied in frequency and
time domains. Obtained results show that the antenna can achieve
a bandwidth of 118% from 2.6–10.1 GHz. The time domain response
of the antenna shows that it has very good time-domain performance.
In addition, the obtained results demonstrate that the antenna has a
good directional radiation in time domain. Therefore, the antenna can
be well applied to ultra-wideband system.

ACKNOWLEDGMENT

REFERENCES

1. Jahromi, M. N., A. Falahati, and R. M. Edwards, "Bandwidth and
   impedance-matching enhancement of fractal monopole antennas
   using compact grounded coplanar waveguide," *IEEE Trans.
   Antennas Propag.*, Vol. 59, No. 7, 2480–2487, Jul. 2011.
2. Ryu, K. S. and A. A. Kishk, "UWB antenna with single or dual
   band-notches for lower WLAN band and upper WLAN band,"
   IEEE Trans. Antennas Propag., Vol. 57, No. 12, 3942–3950,
   Dec. 2009.
3. Federal Communications Commission, "Revision of part 15 of
   the commission's rules regarding ultra-wideband transmission
   system from 3.1 to 10.6 GHz," 98–153, ET-Docket, Federal
   Communications Commission, FCC, Washington DC, 2002.
4. Schantz, H. G., "Planar elliptical element ultra-wideband dipole
   antennas," *Proc. IEEE Antennas Propagat. Soc. Int. Symp. Dig.*,
   Vol. 3, 44–47, San Antonio, Jun. 2002.
5. Hu, Y.-S., M. Li, G.-P. Gao, J.-S. Zhang, and M.-K. Yang,
   "A double-printed trapezoidal patch dipole antenna for UWB
   applications with band-notched characteristic," *Progress In
   Electromagnetics Research*, Vol. 103, 259–269, 2010.
6. Eldek, A. A., "Design of double dipole antenna with enhance

usable bandwidth for wideband phased array applications," *Progress In Electromagnetics Research*, Vol. 59, 1–15, 2006.

7. Chen, K.-R., C.-Y.-D. Sim, and J.-S. Row, "A compact monopole antenna for super wideband applications," *IEEE Antennas Wireless Propag. Lett.*, Vol. 10, 488–491, 2011.

8. Bahadori, K. and Y. Rahmat-Samii, "A miniaturized elliptic-card UWB antenna with WLAN band rejection for wireless communications," *IEEE Trans. Antennas Propag.*, Vol. 55, No. 11, 3326–3332, Nov. 2007.

9. Akhoondzadeh-Asl, L., M. Fardis, A. Abolghasemi, and G. R. Dadashzadeh, "Frequency and time domain characteristic of a novel notch frequency UWB antenna," *Progress In Electromagnetics Research*, Vol. 80, 337–348, 2008.

10. Sze, J.-Y. and K.-L. Wong, "Bandwidth enhancement of a microstrip-line-fed printed wide-slot antenna," *IEEE Trans. Antennas Propag.*, Vol. 49, No. 7, 1020–1024, Jul. 2001.

11. Liu, W. C. and C. F. Hsu, "CPW-fed notched monopole antenna for umts/imt-2000/WLAN applications," *Journal of Electromagnetic Waves and Applications*, Vol. 21, No. 6, 841–851, 2007.

12. Lu, W.-J., Y. Cheng, and H.-B. Zhu, "Design concept of a novel balanced ultra-wideband (UWB) antenna," *IEEE International Conference on Ultra-wideband* (ICUWB), Vol. 1, 1–4, Nanjing, Sept. 2010.

13. Behdad, N. and K. Sarabandi, "A compact antenna for ultrawide-band applications," *IEEE Trans. Antennas Propag.*, Vol. 53, No. 7, 2185–2192, Jul. 2005.

14. Ghosh, S., B. K. Sarkar, and S. V. Pandey, "TEM horn antenna using improved UWB feeding mechanism," *Proc. European Microwave Conference*, 1398–1401, Amsterdam, Oct. 2008.

15. Mehdipour, A., K. Mohammadpour-Aghdam, and R. Faraji-Dana, "Complete dispersion analysis of vivaldi antenna for ultra wideband applications," *Progress In Electromagnetics Research*, Vol. 77, 85–96, 2007.

16. Fei, P., Y.-C. Jiao, W. Hu, and F.-S. Zhang, "A miniaturized an-tipodal vivaldi antenna with improved radiation characteristics," *IEEE Antennas Wireless Propag. Lett.*, Vol. 10, 127–130, 2011.

17. Song, Y., Y. C. Jiao, T. L. Zhang, G. Zhao, and F. S. Zhang, "Small tapered slot antenna with a band-notched function for wireless applications," *Progress In Electromagnetics Research Letters*, Vol. 10, 97–105, 2009.

18. Cappelletti, G., D. Caratelli, R. Cicchetti, and M. Simeoni, "A low-profile printed drop-shaped dipole antenna for wide-band wireless applications," *IEEE Trans. Antennas Propag.*, Vol. 59, No. 10, 3526–3535, Oct. 2011.

19. Yang, D., J. Pan, Z. Zhao, and Z. Nie, "Desgin of trapezoida cavity-backed resistance loaded bow tie antenna with ultra-wideband and high directivity," *Journal of Electromagnetic Waves and Applications*, Vol. 24, Nos. 11, 121685–1695, 2010.

20. Kwon, D.-H., E. V. Balzovsky, Y. I. Buyanov, Y. Kim, and V. I. Koshelev, "Small printed combined electric-magnetic type ultrawideband antenna with directive radiation characteristics," *IEEE Trans. Antennas Propag.*, Vol. 56, No. 1, 237–241, Jan. 2008.

21. Wang, C.-J. and T.-L. Sun, "Design of a microstrip monopole slot antenna with unidirectional radiation characteristics," *IEEE Trans. Antennas Propag.*, Vol. 59, No. 4, 1389–1393, Apr. 2011.

22. Yeoh, W. S., K. L. Wong, and W. S. T. Rowe, "Wideband miniaturized half bowtie printed dipole antenna with integrated balun for wireless applications," *IEEE Trans. Antennas Propag.*, Vol. 59, No. 1, 339–342, Jan. 2011.

23. Telzhensky, N. and Y. Leviatan, "Novel method of UWB antenna optimization for specified input signal forms by means of genetic algorithm," *IEEE Trans. Antennas Propag.*, Vol. 54, No. 8, 2216–2225, Aug. 2006.

24. Zhang, G.-M., J.-S. Hong, B.-Z. Wang, G. Song, and P. Li, "Design and time-domain analysis for a novel pattern reconfigurable antenna," *IEEE Antennas Wireless Propag. Lett.*, Vol. 10, 365–368, 2011.

25. Diaz Camblor, R., S. Ver Hoeye, C. Vazquez Antuna, G. R. Hotopan, M. Fernandez Garcia, and F. Las-Heras, "Frequency scanning array composed of antipodal linearly tapered slot antennas," *Journal of Electromagnetic Waves and Applications*, Vol. 26, No. 4, 468–479, 2012.

26. Li, R. L., T. Wu, B. Pan, K. Lim, J. Laskar, and M. M. Tentzeris, "Equivalent-circuit analysis of a broadband printed dipole with adjusted integrated balun and an array for base station applications," *IEEE Trans. Antennas Propag.*, Vol. 57, No. 7, 2180-2184, Jul. 2009.

27. Dong, Y. D., W. Hong, Z. Q. Kuai, and J. X. Chen, "Analysis of planar ultrawideband antennas with on-ground slot band-notched structures," *IEEE Trans. Antennas Propag.*, Vol. 57, No. 7, 1886–1893, Jul. 2009.